

The Stress State of the Earth's Lithosphere: Results of Statistical Processing of the World Stress-Map Data

A. I. Koptev^a, A. V. Ershov^b, and E. A. Malovichko^b

^a*OOO Laboratory of Geology and Modeling of Sedimentary Basins (SBmG), Moscow, Russia*

^b*Faculty of Geology, Moscow State University, Moscow, Russia*

e-mail: koptev06@mail.ru, andrey_ershov@list.ru, alena_mob@mail.ru

Received May 16, 2012

Abstract—A method for the statistical processing of the input data on the stress state of the Earth's lithosphere that takes the initial 3-D position of the principle stress axes into account is elaborated. This approach is based on the calculation of the arithmetic mean value for every six independent tensor components during determination of the average stress in any sampling. When determining the sampling for calculation of the average stress for the current cell of the calculated grid, it is proposed to insert the measurements into the sampling that are spatially located in such a manner where the distance from the measurement point to the cell center is less than some value that is named as a search radius. The latter either was specified as a constant for all cells of the calculated grid or was determined assuming that the dispersion of the average tensor was less than some preset value. The results of the application of this approach are presented based on the example of the processing of the measurements from the World Stress Map (Heidbach et al., 2008). The resultant set of the mean stress-field maps reflects the generalized pattern of the stress distribution in the Earth's lithosphere.

Keywords: stress state, statistic processing, search radius, World Stress Map, mean stress field

DOI: 10.3103/S0145875213010067

INTRODUCTION

One of the main disadvantages of any stress-state database in the Earth's crust or lithosphere is the irregular distribution of measurements. When comparing these data with the results of computational modeling, which usually have a regular spatial distribution, this problem is especially acute. Thus, an approach is required that allows the averaging of the data of measurements in areas where their density is relatively high and extrapolation of the information on the regions is characterized by the absence of data or few data.

The first works on averaging of the World Stress Map data at global (Zoback, 1992) and regional (Müller et al., 1992) scales were exclusively qualitative. However, too much subjectivism, which is typical of the visual summarizing of information, does not allow one to consider this method as being sufficiently reliable.

As a result of the statistical processing of the input data, the global map of the stress distribution was firstly presented by D. Coblenz and R.M. Richardson (1995), who used the measurements from the World Stress Map (1992) as input information of 4537 A–C quality. The average orientation of the compression axis for a cell $5^\circ \times 5^\circ$ in size was determined as the mean value of the orientations of the projections on the horizontal plane of the principal compression axes based on the data of measurements that fall into this cell. Among 582 cells with identified orientations, 200

cells contained only one measurement. Thus, the estimation of the dispersion of the calculated mean value made sense only for the remaining 382 cells with two measurements and more. The authors faced a significant problem of an excess of the dispersion of feasible values in 196 of 382 cells (i.e., in more than in half of the cases).

The determination of the average of any value for the current cell of the calculated grid applied in (Coblenz and Richardson, 1995) included only processing of data that fall into this cell and may be considered as corresponding to the use of constant search radius (about 250 km in the given case). Hereafter, the search radius is some value that determines the maximum distance from the center of the current cell of the calculated grid to the projection on the horizontal plane of the point of the current measurement from the applied database, the non-exceedance of which allows the presence of this measurement in the sampling for the determination of the mean stress value for the reviewed cell.

The high dispersions for significant numbers of cells with identified average orientations of the compression axes are considered to be related to the use of a constant search radius for all cells of the calculated grid (Coblenz and Richardson, 1995). Thus, later (Heidbach et al., 2007, 2010) it was suggested that one should average different grid cells with different radii.

The search radius of the current cell was consecutively sorted with a 100-km step in a range from 1000 up to 100 km. The standard deviation of the mean value of the orientation of the compression axis was determined for every radius (contribution of every measurement into the mean value directly depended on its quality and, inversely, on the distance between the location of epicenter of the measurement and the center of the current cell). If this deviation did not exceed the given value, the sorting was stopped and the corresponding search radius was registered for the current cell. Thus, the output contained the distribution of the orientation of the principle axes on a regular grid and every element of this distribution was calculated as averaging at a standard deviation that does not exceed the given threshold. Such approach considers the mean value as a measure of the degree of the irregular stress state of any Earth region.

To reconstruct the stress-state parameters based on the data on earthquake mechanisms, Yu.L. Rebetsky (1999, 2003) suggested cataclastic analysis, which not only determines the orientation of the principal stress axes but estimates the value of maximum tangential stresses and effective thorough pressure. Three stages are distinguished in this method. The first stage is a determination of the orientation of the principal axes of the stress tensor and Lode–Nadai coefficients by selection from all possible stress conditions of such a condition that attains the maximum dissipation of energy accumulated in the elastic deformations. The stress values (to unknown value of the internal cohesion of rocks) are estimated at the second stage of the reconstruction using analysis of the distribution of earthquake mechanisms on the Mohr's circle. The fluid pressure and internal cohesion are calculated at the third stage. The elaborated algorithm was successfully applied to reconstruct the stress field within the western flank of the Sunda subduction zone prior to the Sumatra–Andaman earthquake of 2004 (Rebetsky and Marinin, 2006).

The chief disadvantage of the offered approaches (Coblentz and Richardson, 1995; Heidbach et al., 2010) is that the orientation of the projection on the horizontal plane (principal compression axis) was a value whose average was determined by different methods. At the same time, the main information presented in the World Stress Map is a spatial location of the principle axes of the identified stresses. Thus, the selection of information for the statistical analysis lost a significant part, i.e., only orientation of the horizontal constituent of one of the tensor principle axes was used instead of the complete 3-D stress tensor. As a result, the resultant stress field is two-dimensional (it is possible to characterize only the horizontal constituent of the real distribution) and bears no information about the tectonic regime (predominance of compression, tensile, or shear stresses) in either region. It should be noted that determination of the average stress state was given in (Coblentz and Richardson,

1995). However, the procedure was as follows: some numerical value (from zero for a thrust-fault regime up to 1 for a normal-fault regime) was assigned to every measurement depending on the identified stress state and then these values were averaged for the events that fell into the corresponding sampling. Such an approach may not be considered quite correct.

We offer a statistical analysis of the input data on the stress condition of the Earth's lithosphere that take the 3-D location of the principal stress axes into account and we also present the results of the application of the elaborated approach based on the example of measurements of the World Stress Map (2008) (Heidbach et al., 2008).

METHODS AND INITIAL DATA FOR CALCULATIONS

The suggested method for the processing of the input data is as follows.

The initial data in every measurement bears the spatial location of the principal stress axes represented as the dip azimuth and angle for every axis. Because the stress value on the principal axes is unknown for the majority of measurements in the database, it was decided to use single values on the principal axes of compression and extension stresses (–1 and +1, respectively); the stresses on the intermediate principle axis are considered to be zero. In this case, in the coordinate system where the X axis coincides with the principal compression axis, the Y axis with the intermediate axis, and the Z axis with the principal extension, the stress tensor of any measurement may be written as follows:

$$\sigma' = \begin{pmatrix} -1 & 0 & 0 \\ 0 & 0 & 0 \\ 0 & 0 & 1 \end{pmatrix}. \quad (1)$$

The coordinate system that is common for all measurement included an X axis directed to the north, a Y axis directed to the east, and a Z axis that is radially directed from the Earth's center. In order to obtain the tensor in this coordinate system, it is necessary to carry out the following rearrangement:

$$\sigma_{kl} = \sum_{r=1}^3 \sum_{s=1}^3 \alpha_{kr} \alpha_{ls} \sigma'_{rs}, \quad (2)$$

where σ_{kl} is the current element of the calculated tensor, σ' is the initial tensor, and α_{kr} and α_{ls} are the corresponding elements of the rotation matrix (Kochin, 1965).

The rotation matrix for every tensor is a table of the cosines of angles between the axes of the transformed coordinate systems (Lurie, 1961). If the guide cosines of this matrix are expressed as bedding elements of the principal stress axes, it will appear as follows:

$$\alpha = \begin{pmatrix} \cos(a_z P) \cos(p l P) & \cos(a_z B) \cos(p l B) & \cos(a_z T) \cos(p l T) \\ \sin(a_z P) \cos(p l P) & \sin(a_z B) \cos(p l B) & \sin(a_z T) \cos(p l T) \\ \sin(p l P) & \sin(p l B) & \sin(p l T) \end{pmatrix}, \quad (3)$$

where $a_z P$ and $p l P$ are the dip azimuth and angle of the principal compression axes, $a_z B$ and $p l B$ are the dip azimuth and axes of the intermediate principle axis, and $a_z T$ and $p l T$ are the dip azimuth and angle of the principal extension axis, respectively.

Thus, the suggested approach transforms information about the spatial location of the principal stress axes into the tensor state for all measurements.

Further, in order to determine the mean stress $\langle \sigma_{ij} \rangle$ in any sampling, the mean arithmetic value is calculated for every six independent tensor components:

$$\langle \sigma_{ij} \rangle = \frac{1}{N} \sum_{k=1}^N \sigma_{ij}^k, \quad (4)$$

where σ_{ij}^k is the value of the current element of the stress tensor for the k -th measurement of the sampling and N is the total amount of measurement in the given sampling.

The weight of every measurement in the sampling is the same during determination of the mean value (i.e., it is independent of the quality of the data, the distance from the center of the current cell, and the magnitude of an event).

The spatial orientation of the tensor principle axes was calculated in a standard manner for the visualization and analysis of the resultant mean stress tensor (Mase, 1970).

The most substantial issue here is the identification of the subset of events from a database that exist in the sampling during determination of the mean stress tensor for every cell of the calculated grid. It is suggested that one should input the events into such a sampling whose spatial location is such that the distance from the epicenter (the projection of the measurement point on the horizontal plane) to the cell center is less than some value that was determined above as the search radius.

Two methods for the determination of the search radius value are suggested: in the first case, it was considered to be constant (the models were calculated for radii of 100, 200, 300, 400, 500, and 600 km) and, in the second case, the method was basically similar to that suggested in (Heidbach et al., 2010), i.e., the radius was separately identified for every cell within the range from 2000 to 50 km (the sorting was conducted with a 50-km step) in such a way that the mean dispersion for six independent components of the tensor would not exceed the given value in advance (this value was 0.1, 0.5, or 0.2 in our work). The dispersion s_{ij} of the stress-tensor component was calculated by the following formula:

$$s_{ij} = \frac{1}{N} \sum_{k=1}^N (\sigma_{ij}^k - \langle \sigma_{ij} \rangle)^2. \quad (5)$$

The cell was considered to be complete if the number of measurements in the area determined by the search radius was equal to or exceeded the given value (it was assigned as 1 or 5 for our calculated models). The stress regime identified by this method (thrust, normal, thrust–shear, and normal–shear faults) for every complete cell of the calculated grid was determined from the angle between the principle tensor axes and horizontal plane according to the classification accepted in the World Stress Map.

As input information, we used all the measurements from the World Stress Map (2008) that have data on the location of the principle stress axes with a quality no less than category C. It should be emphasized that the release of the World Stress Map (2008) contains 21 750 measurements, which is almost three times higher than of the World Stress Map of 1992. Approximately 17 000 measurements correspond to the A to C quality category (i.e., the orientation of the projection on the horizontal plane of the principle compression axis was determined with an accuracy no less than $\pm 25^\circ$ for all these measurements). In contrast to (Heidbach et al., 2010), data that are marked as measurements that correspond to plate boundary events (PBEs) were not excluded from consideration. The cells of the calculated grid were $1^\circ \times 1^\circ$ in size.

It should be noted that the initial data on focal mechanisms are kinematic, i.e., during direct calculation, they allow us to obtain the parameters of the tensor of the recoverable elastic deformations in areas of the corresponding earthquake focuses. Thus, it should be remembered that transition from these data to the tensor of the recoverable stresses is possible only if the media is characterized by elastic isotropic properties.

RESULTS AND DISCUSSION

Figure 1 shows the results of processing the World Stress Map data that were obtained for a variable search radius that was determined from the conditions that the dispersion of the mean tensor does not exceed 0.15 (the minimum possible amount of events is 5). Among all calculated model, precisely this one obtained at such conditions most specifically reflects the stress-state pattern of the Earth's lithosphere. The boundaries of lithospheric plates on Figure 1 and other figures are based on the digital model of P. Bird (2003).

The following major peculiarities may be distinguished in the stress field:

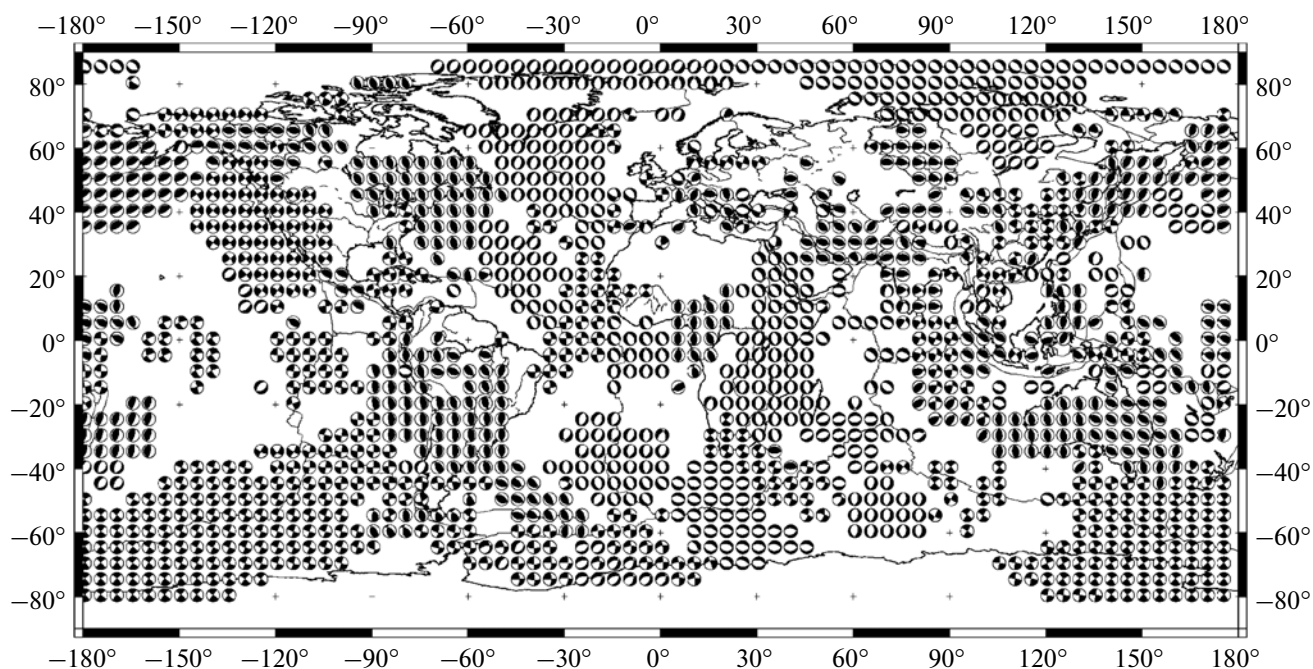


Fig. 1. The results of statistical processing of the World Stress Map data (the maximum permissible dispersion is 0.15 and the minimum number of events is 5). The averaged stress tensors are given as a “beachball plot” (nodal planes in a stereographic projection onto the lower semisphere).

(1) The normal-fault stress type dominates along the spreading boundaries and adjacent intraplate oceanic areas, excluding the East-Pacific and Australia–Antarctic mid-oceanic ridges, which are mostly characterized by a shear fault regime;

(2) A normal fault regime is clearly observed in the East-African, Red Sea, and Baikal rift systems. We should note that the orientation of the principal extension axes both in oceanic and continental divergent boundaries is nearly always transverse to their strike;

(3) The thrust style of the stress state is well expressed in the subduction zones of the western part of the Pacific ocean (Japan and Kuril–Kamchatka) and the central part of the Andes subduction zone and the principal compression zones are oriented transversely to the convergent margins;

(4) Shear stresses prevail in the southwestern part of the North America (the area of the San-Andreas fault);

(5) Thrust stresses with mainly near-latitudinal (locally, up to northwestern–southeastern) orientation of the principal compression axes are developed in the northeastern part of North America and the central part of Africa and South America;

(6) All of Australia is under the influence of thrust stresses; the principal compression axes change the near-latitudinal strike in the western part of the continent to the northeast in the east;

(7) Thrust stress that is characterized by a near-longitudinal orientation of the principal compression

axes is widespread in the northwestern part of North America and the central part of Eurasia.

As was indicated above, the search radius value that was identified for every complete calculated grid determines the degree of homogeneity of the stress state. Thus, the stress field of the regions that are characterized by low values of the search radius is considered to be carried by forces that are related to local density heterogeneities and active fault systems. The areas of lithosphere with a large search radius that were used during the calculation of the mean stresses are believed to be regions where the stress state is mainly controlled by so-called forces of plate boundaries that are delivered at a large distance into intraplate areas. However, such a contradiction between intralithospheric and boundary forces is not quite correct because, for example, the ridge-push forces (presented as an example of boundary forces), in fact, are special case of forces of the difference of the gravitation potential related to the density heterogeneities inside the lithosphere (i.e., intralithospheric forces (Heidbach et al., 2010)). During numerical modeling of the stress field in the Earth’s lithosphere, the ridge-push forces are not related to oceanic rift systems but are distributed along the entire oceanic lithosphere and are calculated by the same scheme as forces of density heterogeneities on the continents (Koptev and Ershov, 2010).

Using shades of gray, Fig. 2 shows the search radius that is used during calculations of the mean stresses that were discussed above and shown on Fig. 1. It is

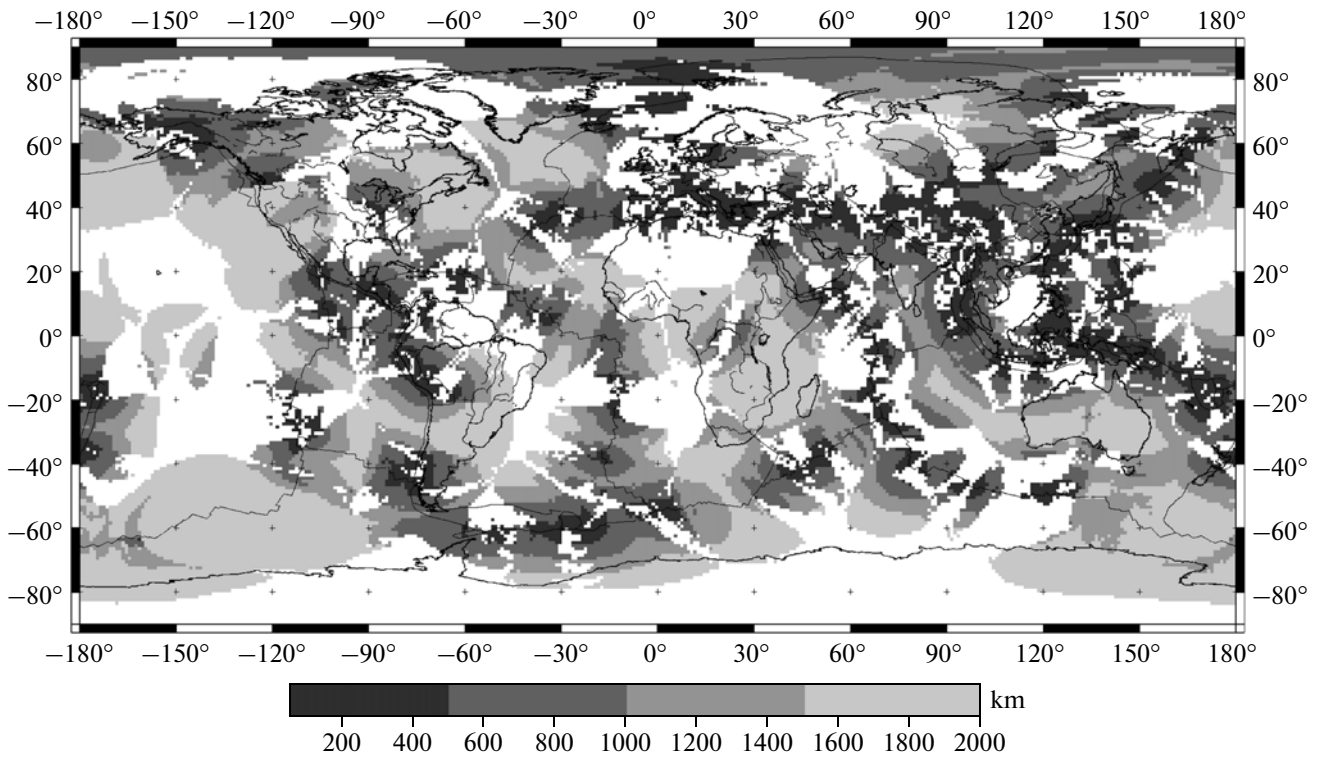


Fig. 2. The search radius that was used during the calculation of the mean values of the stress tensors that are shown on Fig. 1.

seen from Fig. 2 that the largest heterogeneity of the lithospheric stresses is located in the Alpine–Himalayan foldbelt, along the majority of subduction boundaries (excluding the central part of the Andes zone), and in some areas of the worldwide rift system. A more homogeneous stress distribution is seen in Australia, most of Africa, North and South America, and a significant part of the World Ocean.

In discussing the dependences of stress distributions that resulted from statistical analysis on the parameters of this processing (a constant or variable search radius, the minimum possible amount of measurements with determination of the mean values of tensor components, and the maximum possible dispersion in the selection of the search radius), the following patterns may be distinguished.

For a constant search radius, those cells are found to be complete that directly adjoin (i.e., are located at a distance no larger than the given radius) to the areas with a significant quantity of measurements. The measurements from the World Stress Map are mainly concentrated along the plate boundaries but intraplate areas exist that are characterized by a considerable density of measurement (for example, Australia, the western part of North America, Europe, etc.). An increase in the search radius from 100 to 600 km produces a regular and gradual increase in the number of complete cells. The results of calculations within one search radius weakly depend on the given minimum

possible amount of measurements (1 or 5). The difference is relatively notably manifested only for the internal part of the Pacific plate with single measurements in areas of modern plume magmatism which allow us to complete corresponding cells in one case, and do not allow it in another case.

If the search radius for every cell was determined when the dispersion of the mean tensor does not exceed the assigned value (0.1, 0.15 or 0.2), a rather high sensitivity of the final distribution is noted for this parameter: the higher the value of the possible dispersion, the lower the incomplete cells in the calculated grid are and the higher the degree of generalization is upon averaging of the input data. The effect of the minimum possible number of measurements is most intensely manifested at the minimum value of the possible dispersion (0.1). First of all, this is reflected in a significant decrease in the number of complete cells upon an increase from 1 to 5.

Generally, the processing of measurements of the stress state, assuming that the dispersion of the average stress tensor in every complete cell of the calculated grid does not exceed some value given in advance, is preferable in comparison with the constant search-radius method. This is related to the fact that during determination of the work sampling using a constant radius the mean values for different cells are characterized by different dispersions; consequently, they can-

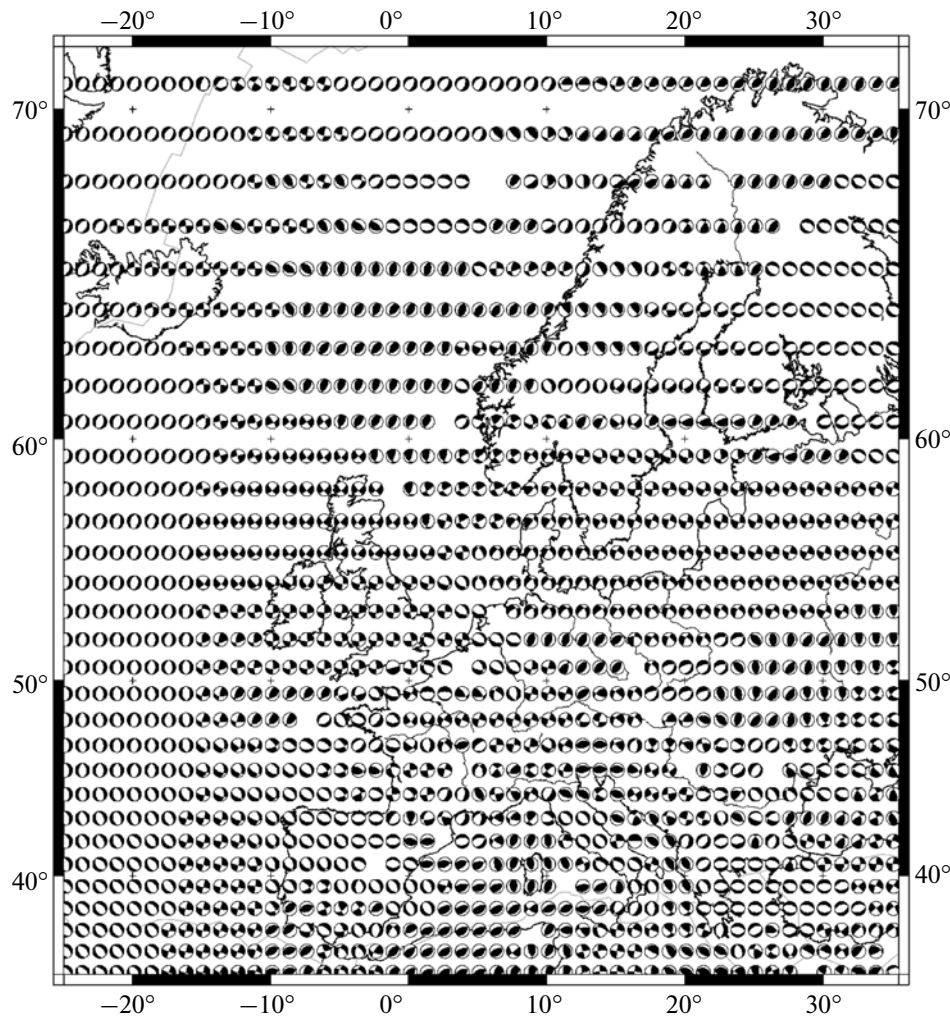


Fig. 3. The results of the statistical processing of the World Stress Map data for the European region (the maximum permissible dispersion is 0.15 and the minimum number of events is 1). The averaged stress tensors are given as a “beachball plot” (nodal planes in a stereographic projection onto the lower semisphere).

not be considered as homogeneous information (this information has different degrees of reliability).

The possibilities of the elaborated method are demonstrated based on the example of the European region (an area limited by meridians at 25° W and 25.5° E and by parallels at 34.25° N and 71.5° N). The resolution of the calculations in this case was 0.25° × 0.25°.

The same set of models and parameters that were used in the case of global calculations (see above) was calculated for Europe, except that the search radius varied from 2000 to 10 km (with a 10-km step) rather than from 200 to 50 km (with a 50-km step) but in regard to a decrease in the cell size of the calculated grid, it was necessary to decrease the minimum possible radius and, respectively, the step of the selection.

In addition, the sensitivity of the results to the range and the step of selection of the search radius were calculated. In particular, we calculated the complete set of models for a 25-km step of selection and

the same minimum value of the range of selection. As a result, it was established that high sensitivity does not occur for these parameters, i.e., their relative low variations do not lead to significant changes in the input data.

Figure 3 shows the results that correspond to the maximum permissible dispersion of 0.15 at the minimum permissible number of events of 1.

The following peculiarities of the distribution were revealed:

- (1) Generally, shear stresses are dominant in the continental part of Europe;
- (2) The orientation of the axes of the minimum stresses in the continental part of Western Europe is northwestern—southeastern to north—northwestern to south—southeastern;
- (3) An extension is observed at the Western Anatolia and Balkan Peninsula where the principal axes have mostly a near-longitudinal orientation, in Apennines

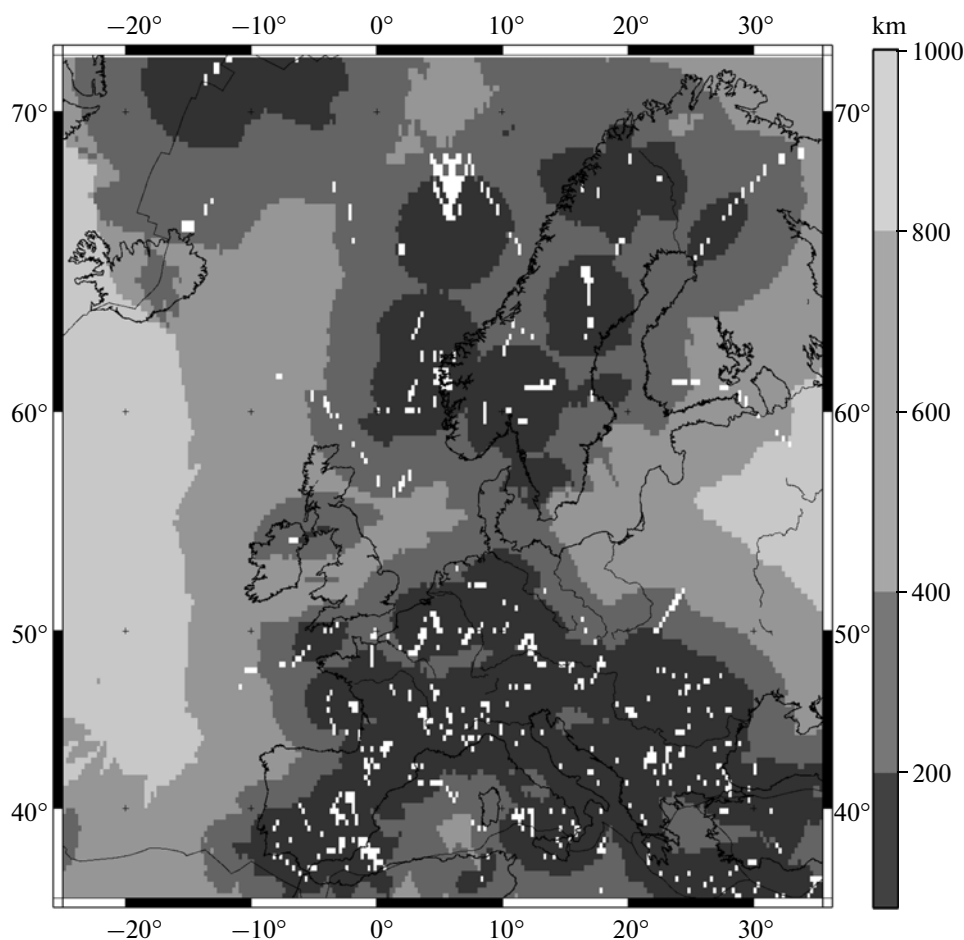


Fig. 4. The search radius that was used during calculation of the mean values of the stress tensors that are shown in Fig. 3.

and Karelia where the strike of the principal extension axes is northwestern–southeastern, and in the Pyrenean Peninsula where the orientation of the axes of maximum stresses varies from near-longitudinal to near-latitudinal;

(4) Thrust stresses are widespread in the Pyrenees and Alps where the principal compression axes vary extremely in orientation (from near-latitudinal to near-longitudinal) and in the northern part of Northland and the North Sea where the minimum stress axes have a northwestern–southeastern (to west-northwestern–east-southeastern) strike;

(5) The compression is dominant in the western part of the Mediterranean, Tyrrhenian, Adriatic, and Ionic seas, whereas a near-longitudinal extension prevails in the Aegean Sea.

The distribution of the search radius that is used for statistical estimation of the average stresses in Europe is shown in Fig. 4. Its major features are:

(1) The search radius is no higher than 800 km within almost the entire continental part of the reviewed area (excluding the very eastern area that corresponds to the East-European platform);

(2) Most of the European part of the Alpine–Hercynian foldbelt has low values (<200 km) of the search radius, whereas it attains 500 km only in the very northern part of the Pyrenean Peninsula and British Isles;

(3) An search radius from 200 to 400 km is typical of the eastern part of the Mediterranean, Ionic, and North seas but in some areas it exceeds 400 km;

(4) The search radius in Northland varies quite irregularly from 100 to 600 km;

(5) The zone of rapid transition is outlined from areas with relatively low search radius (<200 km) on the west to zones of comparatively high values (>400 km) on the east. This zone extends approximately along the Tornquist–Teisseyre Line.

The general variations in the calculated results that depend on the input parameters of the statistical processing for Europe have the same major peculiarities that were established and described for the global average stress field (see above).

The complete list of our results (both at the global scale and for the European region) is available at

<http://sbmg.geol.msu.ru/pp/akoptev> (or <http://www.koptev.lgb.ru>).

The results of statistical processing of the World Stress Map data are used for the qualitative estimation of the degree of correspondence between the input data and numerical models of the stress state of the Earth's lithosphere. The method that was used for the construction of these models and calculated results are presented in (Koptev and Ershov, 2008, 2011; Koptev et al., 2009, 2010). Usually, the degree of coincidence of the deformation regime (the percentage portion of the coincidences relative the total number of comparative points) and/or mean-square difference of angles between the principle axes of calculated and observed stress tensors are used as a criterion of the coincidence between the calculated and input data (Burbidge, 2004; Liu and Bird, 2002).

We suggest an alternative criterion. Three squares of differences between the independent horizontal components of the calculated and input tensor (averaging tensor implied input one) were calculated for every cell that was completed as a result of averaging of the World Stress Map data. The mean value of these squares determines the degree of correspondence between the model calculations and those observed in the current cell. Such an approach allows us to obtain a more independent and objective measure of the correspondence of model constructions and the observed data that is extremely useful not only for the quality estimation of the calculated model but for the correction of the input parameters of future models for results that will more precisely reflect reality.

CONCLUSIONS

We propose a quantitative analysis of the input data on the stress field observed in the Earth's lithosphere that calculates the average arithmetic value for every six independent tensor components when determining the average stress in any sampling. Such an approach takes the initial 3-D position of the principle stress axes into account and not just their horizontal constituent, as was accepted in previous works (Coblentz and Richardson, 1995; Heidbach et al., 2010).

The diversity of the models of the average field of the lithosphere stress that was calculated by this method was determined by different scenarios of distribution by the calculated grid of the search radius, the value of the maximum permissible distance from the center of the current cell to the epicentral point of measurement that falls into the sampling for the current cell. In one case, the search radius was considered to be constant (several models that corresponded to different values were calculated) and in another case it was calculated for every cell when the dispersion of the mean tensor does not exceed some given value (a series of models corresponding to different values of maximum permissible dispersion were calculated).

The results of the processing of the World Stress Map data (Heidbach et al., 2008) demonstrate the abilities of our model during the construction of maps of the generalized stress distribution at both the global and regional scales.

Such a statistical processing method has the main disadvantage of any database on the lithosphere stress state, which is related to the irregular distribution of measurements in the database. The comparison with the results of such an analysis qualitatively estimates the results of the numerical modeling of the stress field, which is extremely useful for the selection of the correct direction of further studies in this area.

This set of maps of the average stress field has independent scientific value because the maps reflect the generalized pattern of the stress distribution in the lithosphere.

REFERENCES

- Bird, P., An Updated Digital Model of Plates Boundaries, *Geochem. Geophys. Geosyst.*, 2003, vol. 4, no. 3, p. 1027. doi:10.1029/2001GC000252
- Burbidge, D.R., Thin Plate Neotectonic Models of the Australian Plate, *J. Geophys. Res.*, 2004, vol. 109, p. 10405. doi:10.1029/2004JB003156
- Coblentz, D. and Richardson, R.M., Statistical Trends in the Intraplate Stress Field, *J. Geophys. Res.*, 1995, vol. 100, no. B10, pp. 20245–20255. doi: 10.1029/95JB02160
- Heidbach, O., Reinecker, J., Tingay, M., Müller, B., Sperner, B., Fuchs, K., and Wenzel, F., Plate Boundary Forces Are Not Enough: Second- and Third-Order Stress Patterns Highlighted in the World Stress Map Database, *Tectonics*, 2007, vol. 26. doi: 10.1029/2007TC002133.
- Heidbach, O., Tingay, M., Barth, A., Reinecker, J., Kurfel, D., and Müller, B., The World Stress Map database release 2008, Paris:, Commission for the Geological Map of the World, 2008.
- Heidbach, O., Tingay, M., Barth, A., Reinecker, J., Kurfel, D., and Müller, B., Global Crustal Stress Pattern Based on the World Stress Map Data Base Release, *Tectonophysics*, 2010, vol. 482, pp. 3–15.
- Kochin, N.E., *Vektornoe ischislenie i nachala tenzornogo ischisleniya* (Vector Calculus and Fundamentals of Tensor Calculus), Moscow: Nauka, 1965.
- Koptev, A. and Ershov, A., Modelling of Global Lithospheric Stress Field on the Spherical Earth, *3rd World Stress Map Conference*, Potsdam, 2008, p. 77.
- Koptev, A.I., Mathematical Modelling of Stress State in the Earth's Lithosphere, *Mat-ly rossiiskoi konf. studentov, aspirantov i molodykh uchenykh "Planeta Zemlya: aktual'nye voprosy geologii glazami molodykh uchenykh"* (Proc. All-Russia Conf. "Planet Earth: Topical Issues of Geology as Viewed by Young Scientists") (Moscow, 2009), Moscow: Mosk. Gos. Univ., 2009, vol. 1, pp. 47–52.
- Koptev, A.I., Computer Model of Stress State in the Earth's Lithosphere, *Mat-ly XLIII Tektonicheskogo soveshchaniya "Tektonika i geodinamika skladchatykh poyasov*

- i platform fanerozoia*” (Proc. XLIII Meet. on Tectonics “Tectonics and Geodynamics of Phanerozoic Fold Belts and Platforms”) (Moscow, 2010), Moscow: Mosk. Gos. Univ., 2010, vol. 1, pp. 356–359.
- Koptev, A.I. and Ershov, A.V., The Role of the Gravitational Potential of the Lithosphere in the Formation of a Global Stress Field, *Izv., Phys. Solid Earth*, 2010, vol. 46, no. 12, pp. 1095–1104.
- Liu, Z. and Bird, P., Finite Element Modeling of Neotectonics in New Zealand, *J. Geophys. Res.*, 2002, vol. 107, no. B12, p. 2328. doi:10.1029/2001JB001075
- Lurie, A.I., *Analiticheskaya mekhanika* (Analytical Mechanics), Moscow: Fizmatlit, 1961.
- Mase, G.E., *Theory and Problems of Continuum Mechanics*, New York: McGraw Hill, 1970.
- Rebetsky, Yu.L., Methods for Reconstructing Tectonic Stresses and Seismotectonic Deformations Based on the Modern Theory of Plasticity, *Dokl. Earth Sci.*, 1999, vol. 365A, no. 3, pp. 370–373.
- Rebetskii, Yu.L., Stress-Strain State and Mechanical Properties of Natural Rock Massifs Based on Earthquake Focus Mechanisms and Structural-Kinematic Characteristics of Cracks, *Extended Abstract of Doctoral (Phys.-Math.) Dissertation*, Moscow, 2003.
- Rebetskii, Yu.L., Development of the Method of Cataclastic Analysis of Shear Fractures for Tectonic Stress Estimation, *Dokl. Earth Sci.*, 2003, vol. 388, no. 1, pp. 72–75.
- Rebetskii, Yu.L. and Marinin, A.V., Stressed State of the Earth's Crust in the Western Region of the Sunda Subduction Zone before the Sumatra–Andaman Earthquake on December 26, 2004, *Dokl. Earth Sci.*, 2006, vol. 407, no. 2, pp. 321–325.
- Rebetsky, Yu.L. and Marinin, A.V., Preseismic Stress Field before the Sumatra–Andaman Earthquake of 26.12.2004: a Model of Metastable State of Rocks, *Geol. Geofiz.*, 2006, vol. 47, no. 11, pp. 1192–1206.
- Zoback, M.L., First and Second Order Patterns of Stress in the Lithosphere: The World Stress Map Project, *J. Geophys. Res.*, 1992, vol. 97, pp. 11703–11728.
- Müller, B., Zoback, M.L., Fuchs, K., Mastin, L., Gregersen, S., Pavoni, N., Stephansson, O., and Ljunggren, C., Regional Patterns of Tectonic Stress in Europe, *J. Geophys. Res.*, 1992, vol. 97, pp. 11785–11803.